Organic modification of mesoporous silicon rugate filters: the influence of nanoarchitecture on optical behaviour

Kristopher A. Kilian

School of Chemistry,
University of New South Wales,
Sydney 2052, Australia
E-mail: k.kilian@student.unsw.edu.au

Till Böcking

School of Chemistry and School of Physics,
University of New South Wales,
Sydney 2052, Australia
E-mail: t.boecking@unsw.edu.au

Leo M.H. Lai

School of Chemistry,
University of New South Wales,
Sydney 2052, Australia
E-mail: z3099262@student.unsw.edu.au

Suhrawardi Ilyas

School of Physics,
University of New South Wales,
Sydney 2052, Australia
E-mail: suhra@phys.unsw.edu.au

Katharina Gaus

Centre for Vascular Research,
University of New South Wales,
Sydney 2052, Australia
E-mail: k.gaus@unsw.edu.au

Michael Gal

School of Physics,
University of New South Wales,
Sydney 2052, Australia
E-mail: m.gal@unsw.edu.au

J. Justin Gooding*

School of Chemistry,
University of New South Wales,
Sydney 2052, Australia
E-mail: justin.gooding@unsw.edu.au
*Corresponding author

Abstract: The internal nanostructure and optical properties of mesoporous silicon rugate filters prepared on different p^+ type silicon substrates are compared for applications in biosensing. Chemical derivatisation of the internal surface by undecenoic acid hydrosilylation results in red-shifting of the resonant wavelength of the filter, whereby the magnitude of the red shift is found to be a function of the pore morphology. The pore structure was found to play a significant role during infiltration of protein into the photonic crystal.

Biographical notes: Kristopher A. Kilian received Bachelor and Masters Degrees in Chemistry from the University of Washington in Seattle, WA. He is currently in the final year of his PhD at the University of New South Wales under the supervision of Professor J. Justin Gooding in Chemistry with co-supervision by Michael Gal in Physics. His research interests involve chemical and biological modifications of photonic structures for advances in novel composite materials, biosensing transducers and components of medical devices.

Till Böcking completed his PhD studies in Biophysics and subsequently joined the research groups led by Justin Gooding and Michael Gal at the University of New South Wales as a Postdoctoral Research Associate to work on the functionalisation of porous silicon based photonic crystals. He is currently a Postdoctoral Fellow at the Harvard Medical School where his research interests include modification of materials and interfaces by self-assembly to develop tools for investigating biological processes.

Leo M.H. Lai is a PhD student at the University of New South Wales, School of Chemistry under the supervision of Professor J. Justin Gooding. He completed his Bachelor and Honours Degrees in Nanotechnology at the University of New South Wales. His current research focus is on superparamagnetic gold nanoparticles for biological and medical applications.

Suhrawardi Ilyas is a Postgraduate PhD student in the School of Physics at the University of New South Wales in Sydney Australia. His research area is in the design and fabrication of porous silicon based optical devices. He holds an Undergraduate Physics Degree from the Institute of Technology Sepuluh, Indonesia and a Masters Degree in Physics from the University of New South Wales.

Katharina Gaus is the Leader of the Membrane Cell Biology group at the Centre for Vascular Research, University of New South Wales and her research focuses on membrane organisation (lipid rafts) in signal transduction processes. Since receiving her PhD in 1999 from the University of Cambridge, she has been granted research fellowships and research grants from the Australian Research Council, Australian National Health and Medical Research Council and the Australian National Heart Foundation. To date, she has published 32 papers in international peer reviewed journals including in *PNAS, J. Cell Biol., EMBO J., FASEB J* and *J. Chem. Biol.*

Michael Gal is a Professor of Physics at the University of New South Wales. He has worked as an academic for 35 years teaching in Europe, the USA and Australia and has been a Research Leader in the field of Semiconductor Optics. He is the author of approximately 200 peer-reviewed publications, two textbooks and he is a fellow of the Institute of Electrical and Electronics Engineers (IEEE).

J. Justin Gooding is a Professor of Chemistry and the Leader of the Laboratory for Nanoscale Interfacial Design at The University of New South Wales. He obtained a DPhil from Oxford University under the guidance of Professor Richard Compton before becoming a Post-Doctoral Research Associate at the Institute of Biotechnology at Cambridge University. In 1997, he returned to his native Australia as a Vice-Chancellor Post-Doctoral Research Fellow at the University of New South Wales before taking up an academic position in 1998. His research interests are in monolayer modification of surfaces to give the surface a desired functionality, electron transfer kinetics, electrochemistry, biosensors and biomaterials.

1   Introduction

The past decade has seen an explosion of interest in the field of photonic materials. Photonic crystals are materials with a photonic 'band-gap' that determines the propagation of light in the material [1]. The photonic band-gap, in turn, is a sensitive function of the refractive index of the material and hence photonic crystals can be used as sensors capable of revealing small changes in the composition. In this study, we have used photonic crystals made from porous silicon. Porous silicon (PSi) photonic crystals are easily fabricated, are amenable to conventional semiconductor fabrication procedures, and importantly for this study, have large internal surface area that can be used as a convenient platform to study surface chemistry. For these reasons, PSi photonic crystals have been explored in the past in various optical applications, including sensors [1–3], micro-cavities [4] and filters [5–7]. One type of filter, which is often used as an optical sensor is the rugate filter. Rugate filters are photonic crystals with a sinusoidal varying refractive index, which results in an optical spectrum characterised by a single, narrow, high reflectivity (resonant) line. The principle of operation for some rugate filter based devices relies on the infiltration of gases, liquids and organic or biological material into the pores of the material, resulting in a shifting of the resonant frequency.

Chemical modification of the internal surface area of PSi photonic materials is necessary for specific capture of biomolecules. In addition, exposure to aqueous environments requires chemical modification to protect the hydride-terminated silicon after anodic etching from attack by water. Alkene hydrosilylation chemistry provides

a method to covalently tether an organic species to PSi without an intervening silicon dioxide layer and provides unparalleled stability of the attached chemical moieties through Si-C bonds [8]. Additionally, providing ω-chemical functionality to the alkene allows subsequent coupling steps to form covalent multilayers for constructing biointerfaces [9–11].

The purpose of this work is to assess the structural and optical qualities of PSi rugate filters for use as biosensing transducers. Rugate filters formed on substrates of two different doping concentrations are prepared to exhibit a narrow resonant linewidth as described previously [7] with some modifications to the etching parameters made to maximise the magnitude of the reflectivity stop-band while minimising the full-width half maximum and background reflectance. Undecenoic acid monolayers provide a stable surface bound organic species to protect the substrate whilst providing ω-functionality for covalent coupling of other molecules to the distal carboxylic acid [12]. The effect of organic material on the optics is analysed in detail and discussed with respect to the observed characteristics of the different materials.

2   Results and discussion

To compare the structural characteristics of the two mesoporous materials, scanning electron micrographs (SEM) were collected. Figure 1(a) is a cross-section of the moderately doped porous silicon ($p^+_{0.07}Si$ – resistivity 0.07 Ω cm). The morphology of this material contains a highly branched network of pores unlike the more commonly reported columnar structures [13]. Earlier studies reported that p^+ porous silicon layers fabricated in this doping regime display similarly branched morphological characteristics with pore sizes typically <10 nm [14]. Increasing the doping and current density was shown to lead to the gradual formation of regular column-like pore structures with 20 nm < pore diameter < 50 nm. The SEM of the highly doped porous silicon ($p^+_{0.005}Si$ – resistivity 0.005 Ω cm) fabricated at a higher current density closely conforms to a columnar porous morphology with average pore sizes of ~50 nm as expected (Figure 1(b)). Although there are distinct differences in pore morphology, since the porosity is similar (theoretical porosity 50–60%), we would expect the optical characteristics of the two materials to be comparable (refractive index is influenced by porosity which determines the position of the reflectivity stop-band). The large difference in pore size for the same porosity means that the $p^+_{0.07}Si$ has a much larger silicon surface area for the same volume of material.

After PSi formation, the optical properties of the two materials were compared. Figure 2(a) and (b) demonstrates the high reflectivity and narrow-linewidth obtained with both types of silicon (black) [7]. Hydrosilylation of undecenoic acid on PSi was performed to demonstrate a methodology for adding chemical functionality to the surface (Figure 2(c)). Optical assessment after monolayer formation demonstrated red shifting of the high reflectivity stop-band for both materials as shown in Figure 2 (red). The $p^+_{0.07}Si$ reflectivity after organic derivatisation shifted 95 nm maintaining a FWHM of 14–18 nm. Inspecting the $p^+_{0.005}Si$ optics upon derivatisation, a much smaller reflectivity shift of 28 nm with the FWHM maintained at 19–20 nm was observed.

Figure 1   Scanning electron micrographs gathered using a Hitachi S900 SEM of (a) moderately boron doped porous silicon ($p^+_{0.07}Si$) etched on 0.07 Ω cm wafer and (b) highly boron doped porous silicon ($p^+_{0.005}Si$) etched on 0.005 Ω cm wafer
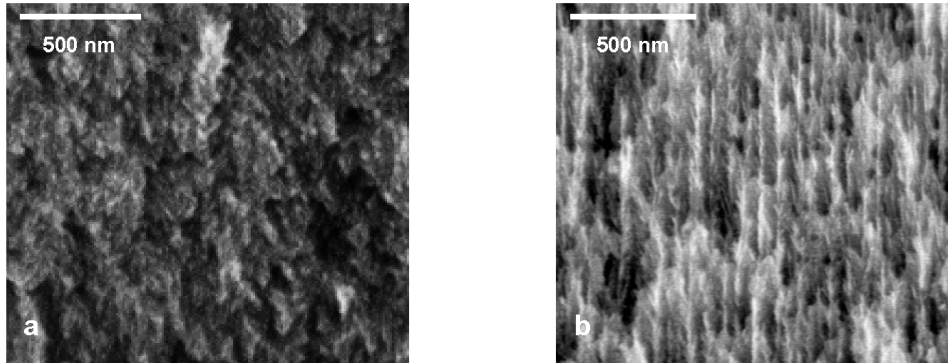

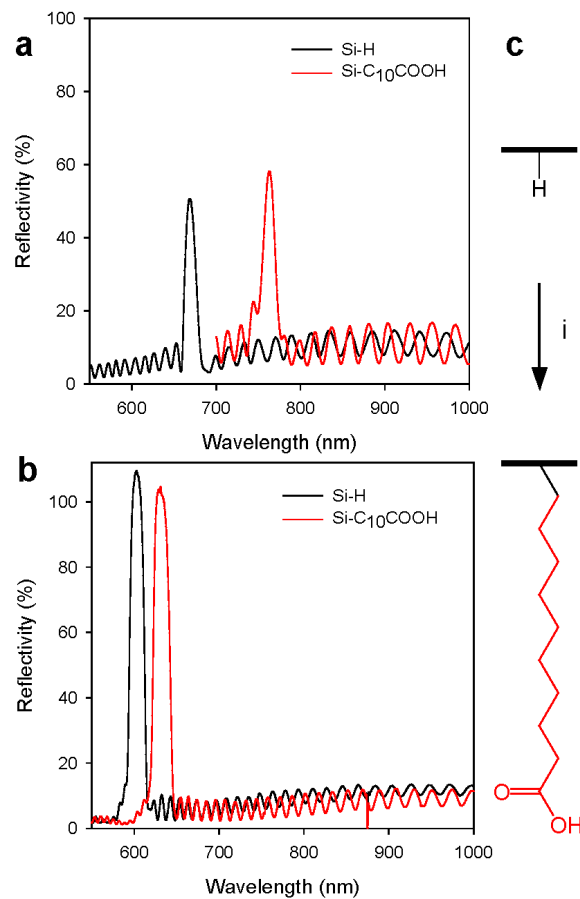**Figure 2**   Porous silicon rugate filter reflectivity profile for (a) medium doped porous silicon ($p^+_{0.07}Si$) and (b) highly doped porous silicon ($p^+_{0.005}Si$) before (black) and after (red) hydrosilylation of undecenoic acid (c). (i) Freshly etched PSi samples were reacted at 120°C for 20 h in degassed 33% undecenoic acid in mesitylene (v/v) under argon

The difference in optical shift can be attributed to the different pore size of the two materials (Figure 1). The reflectivity shift is a consequence of the monolayer on the PSi surface having a different refractive index to air, which changes the average refractive index of the material. The smaller the pore, the larger the quantity of internal pore volume that is replaced by the higher refractive index organic molecules (the monolayer) and hence, the larger the optical shift. Therefore, in the core of the $p^+_{0.07}Si$ (pore size ~10 nm), considerably more of the air is replaced by the organic molecules of the monolayer (than the $p^+_{0.005}Si$ – pore size ~50 nm) and hence, the greater the shift in the reflectivity. If this hypothesis holds true, filling the pores entirely (not merely the walls) with solvents of different refractive index should result in comparable optical shifts for similarly porous materials (irrespective of pore morphology), thus providing a true measure of porosity.

To confirm this hypothesis and further evaluate the optical characteristics of the materials both types of PSi were immersed in a range of solvents and the reflectivity spectrum measured. Figure 3 shows the linear relationships between refractive index change and reflectivity shift. Both materials have very similar optical shift response upon solvent infiltration for the freshly etched rugate filters. The slope of the solvent curves is directly proportional to the material's porosity. For both freshly etched materials the slopes are approximately equal (freshly etched: $p^+_{0.07}Si$ slope/$p^+_{0.005}Si$ slope = 1.07), enough to infer that the actual porosity is comparable between both freshly prepared materials.

Figure 3   Solvent curves demonstrating the linear relationship between changes in high reflectivity stop –band and average refractive index in the porous silicon rugate filters. Black lines represent freshly etched PSi and red lines after organic derivatisation with undecenoic acid. Air ($n = 1.000$), pentane ($n = 1.358$), dichloromethane ($n = 1.424$), toluene ($n = 1.496$)
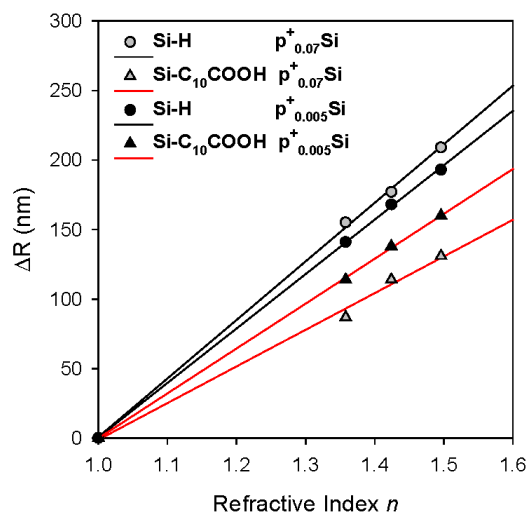

Comparing the slope of the solvent curve for each material before and after organic derivatisation, we see a decrease in the slope after modification consistent with less pore volume available for solvent filling. The slope of the line for $p^+_{0.07}Si$ material decreased from 421 to 264 (change in slope = 158) upon organic derivatisation.

In contrast, the $p^+_{0.005}Si$ material exhibited a smaller change from 392 to 323 (change in slope = 69). Comparing the two materials upon modification we see a greater than two-fold change for the $p^+_{0.07}Si$ material compared to the $p^+_{0.005}Si$ (change in slope $p^+_{0.07}Si$/change in slope $p^+_{0.005}Si$ = 2.29). Therefore, the assertion that material with smaller pores (of the same porosity) will have a greater reduction in pore volume upon monolayer formation is confirmed by this result.

Having elucidated the influence of nanostructure and chemical modification on the optical properties of PSi rugate filters, we turn our attention to the development of these materials for devices. We are interested in using photonic crystals for applications in biology or as device components for biotechnology and medicine. To evaluate the differences between the mesoporous materials towards sensing devices, penetration of biological molecules was evaluated. ^{125}I radiolabelled albumin was incubated on the surface of both materials modified with undecenoic acid and the quantity of adsorbed protein determined. Figure 4 shows the picomoles of protein adsorbed to the $p^+_{0.07}Si$, $p^+_{0.005}Si$ and flat silicon dioxide as control. The $p^+_{0.005}Si$ adsorbed ten times more radiolabelled material than the $p^+_{0.07}Si$ despite the significantly higher surface area (on account of the small pores), which in turn adsorbed approximately three times more than the flat control substrate. The explanation for the large difference in protein adsorption comes from the nanostructural differences observed. Albumin is a relatively large globular protein (44 kDa, ~60–80 nm^3) and the small and branched network of pores observed in the $p^+_{0.07}Si$ limits penetration and diffusion of the molecule. In sharp contrast, the well-defined columnar pores of the $p^+_{0.005}Si$, enables easy diffusion of the biomolecule. A detailed analysis of the size restrictions of these PSi materials for applications in biology will be the subject of a later study.

Figure 4   Comparison of albumin adsorption on porous silicon surfaces; medium doped PSi ($p^+_{0.07}Si$), highly doped PSi ($p^+_{0.005}Si$) and silicon dioxide as control. Protein was labelled with 125-I following the IODO-BEADS™ procedure (Pierce biotechnology) for protein labelling; the concentration was determined using a BCA reagent assay, specific activity determined by using a COBRA auto-gamma and the PSi surfaces were incubated for 4 h in protein followed by copious rinsing with phosphate buffered saline prior to counting
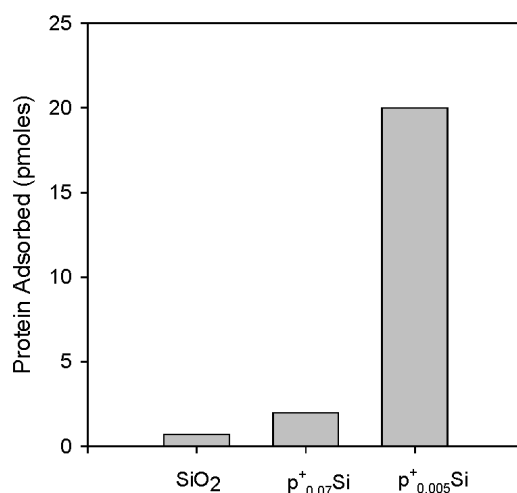
3 Conclusions

We have demonstrated that porous silicon films electrochemically etched on substrates of different dopant concentration display very different nanoscale morphologies. Rugate filters formed by this process display similar optical characteristics as determined by height and width of the high reflectivity stop-band. Organic derivatisation of the material leads to well-defined changes in the position of the stop-band. The magnitude of the shift upon derivatisation was different for the materials and could be explained in terms of pore structure. Infiltration of solvents with different refractive indices showed comparable changes in the optics for freshly etched samples (indicating similar porosities) with a dramatic change upon chemical modification as the smaller pores of $p^+_{0.07}Si$ were filled with organic material. Finally, loading of protein into the porous matrix assessed suitability of this material for use in biosensing. The $p^+_{0.005}Si$ was found to contain much higher quantities of adsorbed biological material most likely due to differences in nanoscale morphology.

The different material properties and well-controlled optical characteristics should allow both types of porous silicon to be integrated into photonic devices. Future work will focus on harnessing the differences between these materials to suit applications with different optical and nanostructural requirements. Employing various chemistry methodologies to functionalise the surfaces of photonic materials will lead to new functional nanomaterials and biophotonic devices and sensors.

Acknowledgements

References

1 Marsh, G. (2002) 'Porous silicon a useful imperfection', *Mater. Today*, Oxford, United Kingdom, Vol. 5, No. 1, pp.36–41.

2 Pacholski, C., Sartor, M., Sailor, M.J., Cunin, F. and Miskelly, G.M. (2005) 'Biosensing using porous silicon double-layer interferometers: reflective interferometric Fourier transform spectroscopy', *J. Am. Chem. Soc.*, Vol. 127, No. 33, pp.11636–11645.

3 Ouyang, H., Christophersen, M., Viard, R., Miller, B.L. and Fauchet, P.M. (2005) 'Macroporous silicon microcavities for macromolecule detection', *Adv. Funct. Mater.*, Vol. 15, No. 11, pp.1851–1859.

4 Reece, P.J., Gal, M., Tan, H.H. and Jagadish, C. (2004) 'Optical properties of erbium-implanted porous silicon microcavities', *Appl. Phys. Lett.*, Vol. 85, No. 16, pp.3363–3365.

5 Lorenzo, E., Oton Claudio, J., Capuj Nestor, E., Ghulinyan, M., Navarro-Urrios, D., Gaburro, Z. and Pavesi, L. (2005) 'Porous silicon-based rugate filters', *Appl. Opt.*, Vol. 44, No. 26, pp.5415–5421.

6 Theiss, W. (1997) 'Optical properties of porous silicon', *Surf. Sci. Rep.*, Vol. 29, Nos. 3–4, pp.91–192.

7   Ilyas, S., Böcking, T., Kilian, K.A., Reece, P.J., Gooding, J.J., Gaus, K. and Gal, M. (2007) 'Porous silicon based narrow line-width rugate filters', *Opt. Mater.*, Vol. 29, No. 6, pp.619–622.

8   Buriak, J.M. (2002) 'Organometallic chemistry on silicon and germanium surfaces', *Chem. Rev.*, Vol. 102, No. 5, pp.1271–1308.

9   Böcking, T., Kilian, K.A., Gooding, J.J., Gaus, K. and Gal, M. (2006) 'Single-step DNA immobilization on antifouling self-assembled monolayers covalently bound to silicon (111)', *Langmuir*, Vol. 22, No. 8, pp.3494–3496.

10   Böcking, T., Kilian, K.A., Hanley, T., Ilyas, S., Gooding, J.J., Gaus, K. and Gal, M. (2005) 'Formation of tetra(ethylene oxide) terminated Si-C linked monolayers and their derivatization with glycine: an example of a generic strategy for the immobilization of biomolecules on silicon', *Langmuir*, Vol. 21, No. 23, pp.10522–10529.

11   Böcking, T., James, M., Coster, H.G.L., Chilcott, T.C. and Barrow, K.D. (2004) 'Structural characterization of organic multilayers on silicon(111) formed by immobilization of molecular films on functionalized Si-C linked monolayers', *Langmuir,* Vol. 20, No. 21, pp.9227–9235.

12   Boukherroub, R., Wojtyk, J.T.C., Wayner, D.D.M. and Lockwood, D.J. (2002) 'Thermal hydrosilylation of undecylenic acid with porous silicon', *J. Electrochem. Soc.*, Vol. 149, No. 2, pp.H59–H63.

13   DeLouise, L.A., Kou, P.M. and Miller, B.L. (2005) 'Cross-correlation of optical microcavity biosensor response with immobilized enzyme activity. Insights into biosensor sensitivity' *Anal. Chem.*, Vol. 77, No. 10, pp.3222–3230.

14   Lehmann, V., Stengl, R. and Luigart, A. (2000) 'On the morphology and the electrochemical formation mechanism of mesoporous silicon', *Mater. Sci. Eng., B*, Vols. B69–70, pp.11–22.